Available online at www.sciencedirect.com
ScienceDirect
Applied Radiation and Isotopes 66 (2008) 168–172
Applied Radiation and Isotopes
www.elsevier.com/locate/apradiso

Determination of biological vector characteristics and nanoparticle dimensions for radioimmunotherapy with radioactive nanoparticles

V.E. Nuttens*, A.-C. Wéra, V. Bouchat, S. Lucas

Laboratoire d'Analyses par Réactions Nucléaires (LARN), University of Namur, 61 Rue de Bruxelles, B-5000 Namur, Belgium

Received 4 May 2007; received in revised form 27 August 2007; accepted 28 August 2007

Abstract

Radioimmunotherapy with biological vector labeled with radioactive nanoparticles is investigated from a dosimetric point of view. Beta (^{32}P, ^{90}Y) and low-energy X-ray radionuclides (^{103}Pd) are considered. Dose distributions inside solid tumors have been calculated using MCNPX 2.5.0. Nanoparticle dimensions and biological vector characteristics are also determined in order to reach the 50 Gy prescribed dose inside the entire tumor volume. The worst case of an avascular tumor is considered. Results show that for beta-emitting nanoparticles, a set of data (covering fraction, biological half-life, and nanoparticle radius) can be found within acceptable ranges (those of classical radioimmunotherapy). These sources (with E_{max}~few MeV) can be used for the treatment of tumors with a maximum diameter of about 1 cm. Low-energy X-rays ($\bar{E}<25$ keV) can be used to extend the range of tumor diameter to 4–5 cm but require very tight biological vector characteristics.

Keywords: Radioimmunotherapy; Biological vector; Radioactive nanoparticles; Dosimetry

1. Introduction

Radiotracers can be used for the treatment of cancerous cells provided that the radionuclide is properly chosen (on the basis of its primary emissions) and that the amount of radionuclide in the vicinity of the tumor is large enough to create lethal damage (Abrams and Fritzberg, 2000; Goldenberg, 2002). Ongoing research into radioimmunotherapy (RIT) aims to provide biological vectors (bV) with increasing uptake (Goldenberg, 2002; Goldenberg et al., 2006). Nevertheless, they are still labeled with only a single radionuclide leading to large amount of drugs injected in the patient. Labeling them with radioactive nanoparticles can circumvent this limitation. Because nanoparticles incorporate thousands of atoms, they are theoretically capable of delivering a larger dose per vector.

However, several challenges have to be won before theory becomes practice. The main challenge is to bind the nanoparticle to a biological vector capable of transporting it to the targeted cells. First, the nature of the material that makes up the nanoparticle will determine its affinity with the biological matter. However, it can be covered by a polymer that would be functionalized with the targeting molecule. In a second step, the biological half-life of the radioactive nanoparticle in the vicinity of the tumor has to be large enough to deliver sufficient dose. The nanoparticle size has an influence on this parameter and on the bV uptake with the corresponding tumor binding site. Indeed, the diameter of the nanoparticle has to be as small as possible in order to reduce the opsonization process by the reticuloendothelial system (RES). Moreover, the polymeric layer covering the nanoparticle could also act as a protective layer against the RES, increasing the biological half-life of the radiopharmaceutics. Uptake will also be increased if the nanoparticle is bound to several biological vectors (identical or different) thanks to the greater number of binding sites per nanoparticle. Furthermore, the binding between a targeting molecule and the radioactive nanoparticle can be broken due to irradiation damage. Therefore, the more biological vectors per nanoparticles there are, the higher will be the biological half-life and bV uptake.

*Corresponding author. Tel.: +32 81 72 54 79; fax: +32 81 72 54 74.
E-mail address: vincent.nuttens@fundp.ac.be (V.E. Nuttens).

0969-8043/$ - see front matter © 2007 Elsevier Ltd. All rights reserved.
doi:10.1016/j.apradiso.2007.08.017

Despite all these challenges, similar assemblies have already been set up and investigated with promising results (Chen et al., 2006; McNeil, 2005; Yokoyama, 2005, Moghimi et al., 2005). Nevertheless, depending on the characteristics of the biological vector (biological half-life and uptake) developed by the pharmacologists, the physicists have to deduce the nanoparticles' characteristics to reach the sufficient prescribed dose.

In this paper, we present a simple model used to determine these parameters in the worst conditions, namely an avascular tumor where radiopharmaceutics are located at the surface of the tumor.

2. Materials and methods

Beta (^{32}P, ^{90}Y) and X-ray (^{103}Pd) emitting nanoparticles have been considered. Because nanoparticles of $^{90}Y_2O_3$ have already been produced experimentally (Xu, 1999), the oxide molecules $^{90}Y_2O_3$ and $^{32}P_2O_3$ have been considered here. Pure ^{103}Pd nanoparticles are considered because they can also be produced (Lucas and Hofferlin, 2007). The characteristics of these three types of nanoparticles are listed in Table 1. Each nanoparticle can be surrounded by a shell containing several biological vectors. In the model considered here, the shell is 15 nm thick (Fig. 1a). The number of biological vectors bound per unit of tumor surface defines the 'covering fraction' f_c (Fig. 1b). Its value depends on the binding characteristics of the targeting molecule and will determine the total activity surrounding the tumor. In the case of monoclonal antibodies (mAb), typical covering fractions range from 10^8 to 10^{10} bV/cm^2 (Howell et al., 1989). Depending on its pharmacokinetics, the biological vector has a limited life due to its clearance from the human body. Biological half-life (T_{bio}) can vary from a few hours to a few weeks (Tobinai et al., 1998; Colnot et al., 2002).

Based on that description, we build a simple geometrical model for the simulation. The solid tumor is a sphere of radius R. The material for the tumor cells is breast tissue from ICRU-44 (ICRU-44, 1989). The biological vector and the nanoparticle are assumed not to absorb any emitted radiation. The whole collection of nanoparticles surrounding the tumor is then modeled by a spherical surface that emits the radiations. The radius of this surface is 15 nm larger than the tumor radius (Fig. 1c).

In a first step, we have studied the distribution of the dose inside the tumor and in the surrounding healthy tissues as a function of the tumor radius. Even if, generally, tumors are vascularized, few data and models are available. We consider therefore the worst case where radiopharmaceuticals are bound at the tumor surface, without any penetration into the tumor (Fig. 1b). Dosimetry results, therefore, give the maximal dose to healthy tissues and the minimal dose to the tumor. If penetration is taken into account, it would increase the dose to the solid tumor and decrease it to healthy tissues.

Dosimetry calculations for nanoparticles of beta (^{32}P, ^{90}Y) and X-ray (^{103}Pd) emitters were performed using

Table 1
Nanoparticle physical characteristics

	$^{32}P_2O_3$ β^- (E_{max} = 1.67 MeV)	$^{90}Y_2O_3$ β^- (E_{max} = 2.23 MeV)	^{103}Pd RX-γ ($\bar{E}$ = 22 keV)
ρ_{molec} (molecule/cm^3)	1.15×10^{22}	1.32×10^{22}	7.03×10^{22}
c_r (at./molecule)	2	2	1
T_{phys} (days)	14.26	2.67	16.991
p (dis^{-1})	1	1	0.7714

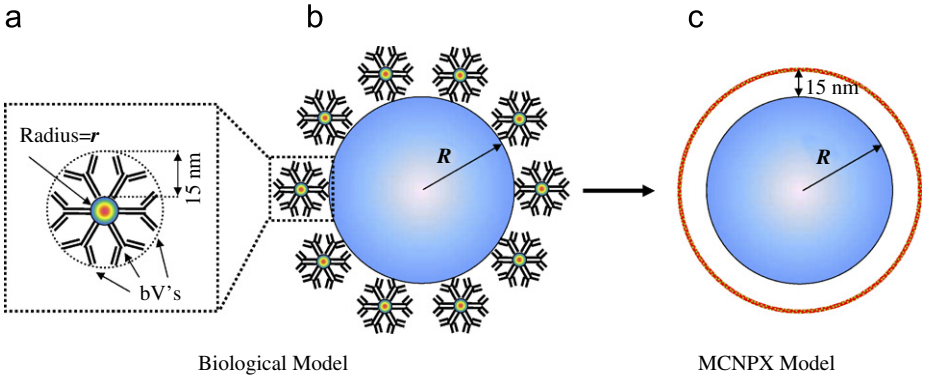

Fig. 1. (a) Schematic representation of a radioactive nanoparticle of radius r bound to several biological vectors. (b) These radiopharmaceutics recover the surface of a spherical tumor of radius R. (c) Simplified model used in MCNPX with the biological medium surrounded by a non-material emitting spherical surface. Not to scales.

MCNPX 2.5.0 (Pelowitz, 2005). The deposited dose was evaluated using the pulse-height tally *F8 modified by a SD card. The ITS energy indexing algorithm was used and energy cutoffs were set to 5 keV. The solid tumor was subdivided into concentric spherical shells of 1 mm thickness, in order to use the tally *F8 for electron dosimetry. Indeed, the spatial resolution for electron dosimetry with tally *F8 should not be higher than $0.85 \times (1-\mathrm{EFAC}) \times$ CSDA, where EFAC is the ratio of adjacent energies in the energy grid for electron cross-section tables used by the code, and CSDA is the electron continuous slowing down approximation range (Reynaert et al., 2002). For 2.5 MeV electrons, the minimal resolution is 0.88 mm.

The radius of the solid tumor was varied from 0.5 to 20 mm. The emitting spherical surface was surrounded by healthy tissues. The dose delivered to these tissues was also calculated, in order to assess the risk incurred by the treatment.

In order to estimate the dose delivered to the tumor and the healthy tissues, the activity (in mCi) at the spherical surface has to be deduced from

$$A = \frac{\lambda_{\mathrm{phys}} n_{\mathrm{a}} n_{\mathrm{bV}}}{3.7 \times 10^{7}}, \tag{1}$$

where λ_{phys} is the radioactive decay constant of the emitter (in h^{-1}). The number n_{bV} of biological vectors that can be bound at the tumor surface is obtained by multiplying the solid tumor surface by the covering fraction. The number n_{a} of radioactive atoms per nanoparticle is $n_{\mathrm{a}} = c_{\mathrm{r}} \times \rho_{\mathrm{molec}} \times 4\pi r^{3}/3$, where c_{r} is the number of radioactive atoms per molecule, ρ_{molec} is the number of molecules per cm^3, and r is the nanoparticle radius.

The deposited dose (in Gy) is obtained with the expression

$$D = \frac{\chi T p A}{\lambda_{\mathrm{eff}}}, \tag{2}$$

where T is the tally value in MeV/g per emitted particle; p (in dis^{-1}) is the average number of particles (electron or photon) emitted per disintegration; A is the activity (mCi); and $\lambda_{\mathrm{eff}} = \lambda_{\mathrm{bio}} + \lambda_{\mathrm{phys}}$ (in h^{-1}) takes into account the decay of the source due to radioactive decay and biological leakage of the radiopharmaceutics. $\chi = 21.34$ is a constant to convert dose rate from mCi MeV/g/dis to Gy/h.

In order to be capable of sterilizing the cancerous cells of the entire solid tumor, a therapeutic dose has to be reached. A minimal value of 50 Gy is generally accepted (Goldenberg et al., 2006). For that purpose, the nanoparticle diameter has to be adapted as a function of the biological half-life and covering fraction of the available biological vectors. Therefore, in the second step, for a specific tumor radius, we determine the covering fraction, the biological half-life of the biological vector and the nanoparticle radius to reach the prescribed 50 Gy throughout the tumor volume.

3. Results and discussions

3.1. Beta emitters: ^{32}P and ^{90}Y

Deposited dose in tumor cells and healthy tissues versus radial distance from the tumor surface are presented in Fig. 2 for $^{90}Y_2O_3$ for various tumor radii. The same overall behavior is observed for $^{32}P_2O_3$ nanoparticles. A fixed nanoparticle radius of 2.5 nm was chosen (1/3 of the biological vector size), and the covering fraction and biological half-life were adjusted to ensure a minimal dose of 50 Gy throughout a 1-cm diameter solid tumor. Due to its short half-life, only 50% of the ^{90}Y atoms are still supposed to be radioactive. T_{bio} has been set to 3 days (Tobinai et al., 1998). Values of 8.91×10^{8} and 5.73×10^{9} bV/cm^2 are obtained for the covering fraction with ^{90}Y and ^{32}P, respectively.

Fig. 2 shows that due to the limited range of electrons in the matter, the dose distribution falls off rapidly when moving away from the radioactive source. It also shows that for a solid tumor of 5 mm radius exposed to ^{90}Y radiation, the doses at the tumor center, 1 mm inside the tumor surface and 5 mm away are, respectively, 54.3, 185 and 5.12 Gy. Outside the tumor, the isodose of 50 Gy is located 1.5 mm away from the tumor surface. A high dose to surrounding tissues is therefore limited to healthy cells close to the tumor volume. In the case of ^{32}P nanoparticles, the corresponding doses are, respectively, 52.6, 619 and 3.28 Gy and the 50 Gy isodose is located 2.5 mm away from the tumor surface. These dose values are much higher than those obtained with bV labeled with only a single radionuclide. For example, Howell et al. (1989) calculated a maximum dose of 7.0 Gy at the surface of a 0.1-cm diameter solid tumor, with mAb labeled with one atom of

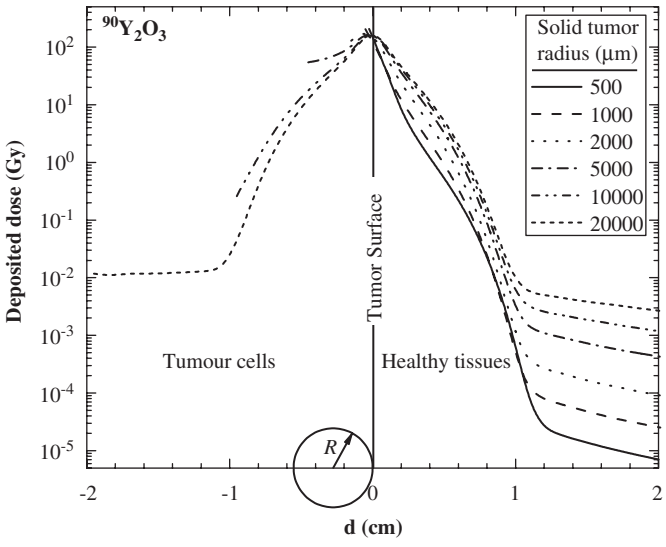

Fig. 2. Deposited dose as a function of distance d from the tumor surface for $^{90}Y_2O_3$ nanoparticles. $d<0$ corresponds to cells in the solid tumor, $d>0$ corresponds to healthy tissues, $r = 2.5$ nm, $T_{\mathrm{bio}} = 3$ days, and $f_{\mathrm{c}} = 8.91 \times 10^{8}$ bV/cm^2.

^{90}Y, the covering fraction being of the same order of magnitude.

The maximum penetration depth of beta particles (CSDA range) emitted from ^{32}P is limited to 8 mm, whereas it reaches 11 mm for ^{90}Y. These differences will have an effect on the range of cell cluster sizes treatable with either radionuclide.

For large solid tumors ($R>$CSDA), the dose will be deposited in a peripheral spherical shell, whose thickness is almost equal to the CSDA range. The inner part of the tumor will not receive a substantial dose and the treatment will not be totally effective. However, for a small tumor ($R<$CSDA), the treatment will be efficient if the dose at each point inside the tumor reaches at least the prescribed dose.

If $2R<$CSDA, the cross-fire effect will lead to deposition of a dose to the surrounding tissues located on the other side of the solid tumor. However, the total activity surrounding the solid tumor is so small that this cross-fire effect does not induce a high dose to surrounding tissues.

The dose background at $d>$CSDA is due to bremsstrahlung photons depositing their energy far away from the cell cluster surface. Its amplitude is proportional to the total activity in all the radioactive nanoparticles surrounding the tumor. However, this contribution to the dose in healthy tissues is negligible. Supposing an avascular tumor, the optimal tumor radius for a treatment with beta emitter would be therefore the half of the CSDA.

Figs. 3 and 4 show the radius of the $^{90}Y_2O_3$ and $^{32}P_2O_3$ nanoparticles required to reach the prescribed dose for different biological half-lives (from 1 h to 30 days) and covering fractions (10^7–10^{11} bV/cm^2) in the case of a 5-mm-radius tumor. For the maximal covering fraction of 10^{10} bV/cm^2 presently available in classical RIT (a single radionuclide per vector), the $^{90}Y_2O_3$ nanoparticle ($^{32}P_2O_3$ respectively) radius can vary from 0.9 nm (1.3 nm) for a biological half-life of 30 days to 3.5 nm (8.0 nm) for a 1-h T_{bio}.

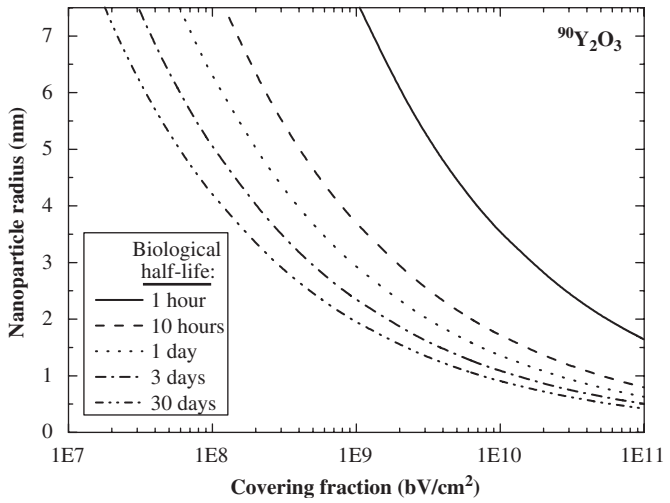

Fig. 3. $^{90}Y_2O_3$ nanoparticle radius as a function of the covering fraction and biological half-life of the biological vector.

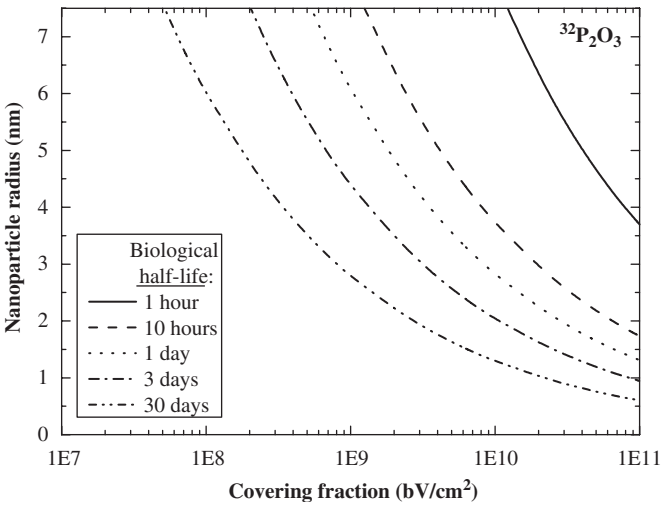

Fig. 4. $^{32}P_2O_3$ nanoparticle radius as a function of the covering fraction and biological half-life of the biological vector.

If, for a fixed covering fraction, pharmacologists manage to set up a bV with a higher T_{bio}, smaller nanoparticles would be required which would make easier the bV transport through the blood to the tumor site. When the covering fraction decreases, the required nanoparticle radius increases or a new biological vector with a longer biological half-life is necessary. Very small nanoparticle size requires therefore higher biological half-lives or higher covering fraction. In conclusion, in order to fulfill the required condition, a synergy is necessary between the physicists and the pharmacologists in the synthesis of biological vectors labeled with nanoparticles.

3.2. X-ray emitter: ^{103}Pd

Due to their limited range in matter, beta emitters are no longer efficient for large solid tumors ($R>5$ mm). In such cases, low-energy X-ray emitters, such as ^{103}Pd are useful. Fig. 5 shows their MCNPX dosimetry results. The ^{103}Pd dose distributions fall off less rapidly than those from the beta emitters. The cross-fire effect gives rise to a high and quite uniform dose inside the solid tumor, whereas, outside the tumor, the dose falls off rapidly. For a 2-cm-radius tumor irradiated by ^{103}Pd nanoparticles, the doses at the solid tumor center, 1 mm inside the tumor surface and 2 cm away are 52.1, 208 and 7.57 Gy, respectively. Outside the tumor, the 50 Gy isodose is located more or less 5.5 mm away from the tumor. However, in order to reach the prescribed dose inside the tumor volume, the nanoparticle size has to be increased to 5 nm in radius, T_{bio} needs to be at least 10 days and, finally, the covering fraction has to be high, 7.64×10^9 bV/cm^2.

Fig. 6 presents the nanoparticle radius needed to reach the prescribed 50 Gy throughout a tumor volume of 2 cm of radius. Compared to ^{90}Y and ^{32}P, very high covering

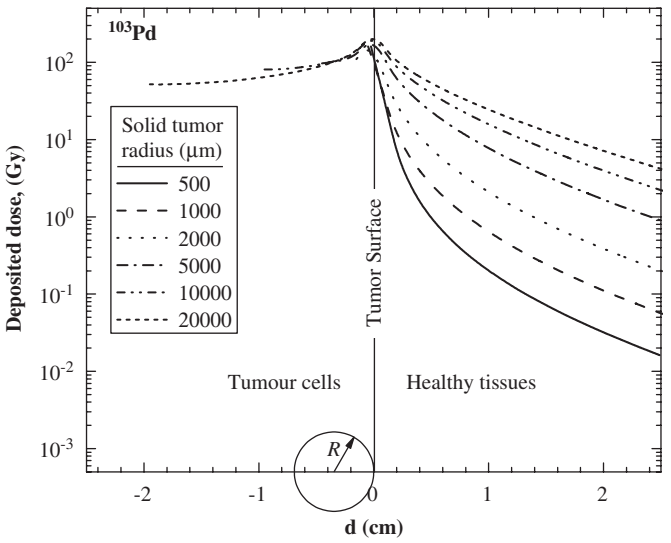

Fig. 5. Deposited dose as a function of distance d from the tumor surface for ^{103}Pd nanoparticles. $d<0$ corresponds to cells in the solid tumor, $d>0$ corresponds to healthy tissues, $r = 5$ nm, $T_{bio} = 10$ days, and $f_c = 7.64 \times 10^9$ bV/cm^2.

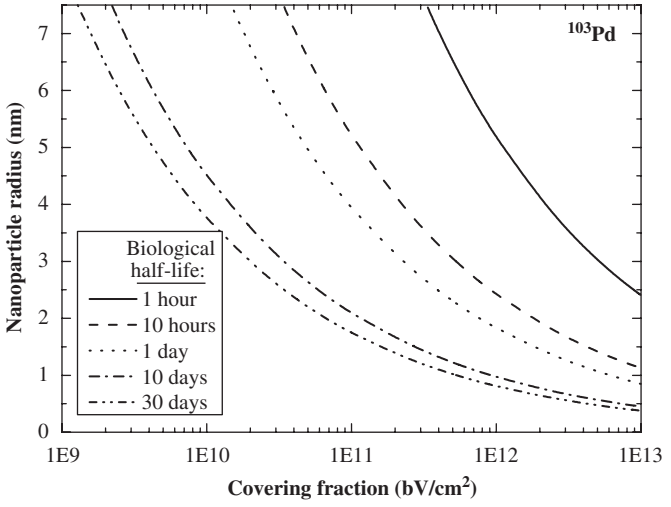

Fig. 6. ^{103}Pd nanoparticle radius as a function of the covering fraction and biological half-life of the biological vector.

fractions are necessary which means that ^{103}Pd nanoparticles deposit less dose per disintegration.

Even if X-ray emitters provide a more homogeneous dose distribution inside the tumor volume, they require very tight biological vector characteristics for nanoparticles of a few nanometer of radius which makes difficult their use in RIT.

4. Conclusions

In this work, we determine the biological vector characteristics and nanoparticle dimensions required to make possible RIT with radioactive nanoparticles. For β-emitters, the optimized tumor radius is equal to half of the CSDA range. For ^{90}Y based nanoparticles, a set of data (covering fraction, biological half-life, nanoparticle radius) can be found within acceptable ranges. For $^{32}P_2O_3$ nanoparticles, higher covering fraction or longer biological half-life are necessary to keep the nanoparticle radius below 7.5 nm. For ^{103}Pd nanoparticles, larger tumor volume can be treated (cm-range in diameter) but very tight conditions on the biological vector are needed. However, this would not exclude the use of X-ray emitters for nanoparticles RIT. Indeed, in our simple model, we consider an avascular tumor. However, if penetration is taken into account, less activity would be required to reach the 50 Gy throughout the tumor volume, which would reduce the nanoparticle radius and the covering fraction and biological half-life of the biological vector.

References

Abrams, P.G., Fritzberg, A.R., 2000. Radioimmunotherapy of Cancer. Marcel Dekker, New York.

Chen, J., Wu, H., Han, D., Xie, C., 2006. Using anti-VEGF McAb and magnetic nanoparticles as double-targeting vector for the radioimmunotherapy of liver cancer. Cancer Lett. 231, 169–175.

Colnot, D.R., Ossenkoppele, G.J., Roos, J.C., Quak, J.J., de Bree, R., Borjesson, P.K., Huijgens, P.C., Snow, G.B., van Dongen, G.A., 2002. Reinfusion of unprocessed, granulocyte colony-stimulating factor-stimulated whole blood allows dose escalation of ^{186}relabeled chimeric monoclonal antibody U36 radioimmunotherapy in a phase I dose escalation study. Clin. Cancer. Res. 8, 3401–3406.

Goldenberg, D.M., 2002. Targeted therapy of cancer with radiolabeled antibodies. J. Nucl. Med. 43, 693–713.

Goldenberg, D.M., Sharkey, R.M., Paganelli, G., Barbet, J., Chatal, J.-F., 2006. Antibody pretargeting advances cancer radioimmunodetection and radioimmunotherapy. J. Clin. Oncol. 24, 823–834.

Howell, R.W., Rao, D.V., Sastry, K.S., 1989. Macroscopic dosimetry for radioimmunotherapy: nonuniform activity distributions in solid tumors. Med. Phys. 16, 66–74.

ICRU-44, 1989. International Commission on Radiation Units and Measurements Report 44, p. 22.

Lucas, S., Hofferlin, E., 2007. Radioactive Rh wire as a source for new nanomaterials. Nucl. Instrum Methods A.

McNeil, S.E., 2005. Nanotechnology for the biologist. J. Leukocyte Biol. 78, 585–594.

Moghimi, S.M., Hunter, A.C., Murray, J.C., 2005. Nanomedicine: current status and future prospects. FASEB J. 19, 311–330.

Pelowitz, D.B., 2005. Los Alamos National Laboratory Report LA-CP-05-0369, Los Alamos.

Reynaert, N., Palmans, H., Thierens, H., Jeraj, R., 2002. Parameter dependence of the MCNP electron transport in determining dose distributions. Med. Phys. 29, 2446–2454.

Tobinai, K., Kobayashi, Y., Narabayashi, M., Ogura, M., Kagami, Y., Morishima, Y., Ohtsu, T., Igarashi, T., Sasaki, Y., Kinoshita, T., Murate, T., 1998. Feasibility and pharmacokinetic study of a chimeric anti-CD20 monoclonal antibody (IDEC-C2B8, rituximab) in relapsed B-cell lymphoma. The IDEC-C2B8 Study Group. Ann. Oncol. 9, 527–534.

Xu, C., 1999. Synthesis of nanometer-sized yttrium oxide particles in diisooctyl sodium sulphosuccinate (AOT)/isooctane reverse micelle solution. Ph.D. Thesis, Blacksburg, VA.

Yokoyama, M., 2005. Drug targeting with nano-sized carrier systems. J. Artif. Organs 8, 77–84.